

RESEARCH ARTICLES

44. M. S. Springer, *J. Mamm. Evol.* **4**, 285 (1997).
45. C. Argot, *J. Morphol.* **248**, 76 (2002).
46. R. L. Cifelli et al., *Nature* **379**, 715 (1996).
47. K. C. Beard, in *Primates and Their Relatives in Phylogenetic Perspective*, R. D. E. MacPhee, Ed. (Plenum, New York, 1992), pp. 63–90.
48. A. Weil, *Nature* **416**, 798 (2002).
49. D. L. Swofford *PAUP*—Phylogenetic Analysis Using Parsimony (*and other Methods)*, version 4.0b (Sinauer, Sunderland, MA, 2000).
50. We thank K. C. Beard, R. L. Cifelli, M. R. Dawson, Z.

Kielan-Jaworowska, J. A. Lillegraven, M. J. Novacek, G. W. Rougier, and M. Sánchez-Villagra for many discussions that are relevant to this research; R. L. Cifelli and M. R. Dawson for improving the paper; A. Henrici and A. R. Tabrum for preparation; and M. Klingler for illustration of Fig. 1. Supported by NSF (USA) (Z.-X.L. and J.R.W.), the Ministries of Land Resources and Science and Technology of the People's Republic of China (Q.J.), NSFC (China) and the National Geographic Society (Z.-X.L.), and the Carnegie Museum of Natural History (Z.-X.L. and J.R.W.).

Supporting Online Material

www.sciencemag.org/cgi/content/full/302/5652/1934/DC1

SOM Text

Figs. S1 and S2

Matrix table (character distribution)

References

PAUP analysis

22 August 2003; accepted 10 November 2003

REPORTS

Subkelvin Cooling NO Molecules via “Billiard-like” Collisions with Argon

Michael S. Elioff,¹ James J. Valentini,² David W. Chandler¹

We report the cooling of nitric oxide using a single collision between an argon atom and a molecule of NO. We have produced significant numbers (10^8 to 10^9 molecules per cubic centimeter per quantum state) of translationally cold NO molecules in a specific quantum state with an upper-limit root mean square laboratory velocity of 15 plus or minus 1 meters per second, corresponding to a 406 plus or minus 23 millikelvin upper limit of temperature, in a crossed molecular beam apparatus. The technique, which relies on a kinematic collapse of the velocity distributions of the molecular beams for the scattering events that produce cold molecules, is general and independent of the energy of the colliding partner.

The development of methods for the preparation and confinement of ultra-cold atoms, with temperatures in the 1 μ K to 1 nK range (1), have made possible the generation of Bose-Einstein condensates (2–4), the observation of atom optics (5), the investigation of collisions at ultra-low energy (6), and the optical clock (7). Ultra-cold atom samples are prepared in a two-step process. Radiation pressure cooling of atoms, via laser light absorption, yields samples at <1 mK, at which temperature the atoms can be held in a magneto-optical or similar trap and the temperature further reduced by optical (8, 9) or evaporative cooling (10).

The preparation and trapping of molecules at similar temperatures has been much desired, although not yet accomplished in a general way (11–13). The radiation pressure cooling that is used as the initial step in the trapping of ultra-cold atoms does not work well for molecules because of their more complex energy-level structure. Other methods for slowing or cooling have been demonstrated to accom-

plish the first step and produce molecules cold enough to be trapped and further cooled. The term “cooling” is reserved for processes that compress the velocity distribution by slowing the particles with higher velocities more efficiently than they slow particles with lower velocities. This process increases the phase space density of the molecules.

Cold molecule production processes include photoassociation of ultra-cold atoms (14–17); adiabatic tuning of a Feshbach resonance in a cold atomic gas (18, 19); and buffer gas loading (20, 21), which uses laser ablation (or molecular beam loading) of a gas into a cold He buffer gas cell wherein bulk collisions cool the molecules in an anti-Helmholtz magnetic trap equilibrated at ~ 1 K. Additionally, varying inhomogeneous electric fields in time has been used to slow molecules (22). In particular, Stark deceleration (23) can slow dipolar molecules to a stop when they have the appropriate Stark behavior. Another technique that has been proposed for slowing molecules is a spinning molecular beam source in which the velocity of the spinning source cancels the velocity of the molecules flowing through it (24). Although successful, each approach has limitations in applicability or execution.

We report here a cooling process for molecules that relies upon a single collision between the molecule and an atom in a crossed molecular beam apparatus that produces molecules with a laboratory velocity that is nominally zero. The technique relies on a kinematic collapse of the laboratory velocity distribution of molecules that are scattered with a particular recoil velocity vector in the center-of-mass (COM) frame. The method depends on the fact that in binary collisions, one of the collision partners can have a final COM-frame velocity that is essentially equal in magnitude and opposite in direction to the velocity of the COM, thus yielding a laboratory-frame velocity that is nearly zero. Cooling occurs because the COM velocity scales with initial NO velocity almost the same as does the recoil velocity.

Only collisions that result in NO molecules recoiling opposite to the direction of the motion of the COM experience the kinematic collapse. NO molecules recoiling in other directions have much larger laboratory velocities and quickly leave the scattering center. Thus, only the NO molecules that have had their velocity distribution narrowed by collision remain. This cooling process is not only general, but it is also realizable under easily accessible experimental conditions in crossed atomic and molecular beams.

The method does not rely on any particular physical property of either colliding species, because zero velocity is a consequence of the experimentally selectable energy and momenta of the collision pair. Moreover, this technique can be used to prepare a single, selectable ro-vibronic quantum state for trapping. We demonstrate this technique using inelastic collisions between NO molecules in one beam and Ar in the other, specifically $\text{NO}(^2\Pi_{1/2,j} = 0.5) + \text{Ar} \rightarrow \text{NO}(^2\Pi_{1/2,j'} = 7.5) + \text{Ar}$. Using an existing crossed molecular beam experimental apparatus that is not specifically optimized for the production of cold molecules, we generate scattered $\text{NO}(^2\Pi_{1/2,j'} = 7.5)$ with a velocity distribution that is centered about zero, with an upper limit root mean square (RMS) velocity of

¹Combustion Research Facility, Sandia National Laboratories, Livermore, CA 94550, USA. ²Department of Chemistry, Columbia University, New York, NY 10027, USA.

15 m s^{-1} . The probability that an atom-molecule collision will result in an NO molecule that is cooled, to within our experimental resolution of approximately 15 m s^{-1} , is small. From an analysis of our data, we estimate that the probability of a molecule having a collision resulting in a velocity less than 15 m s^{-1} is approximately 10^{-5} . In a typical crossed molecular beam experiment, collision frequencies of approximately 10^{13} collisions per second can be achieved. Densities of 10^8 to 10^9 NO molecules cm^{-3} in this single (${}^2\Pi_{1/2}, v', j' = 7.5$) ro-vibrational quantum state (hereafter denoted $\text{NO}_{7.5}$ for convenience) have been achieved.

We use the technique of velocity mapped ion imaging (25–27) to characterize the scattering distribution and density of scattered NO molecules. Our experimental apparatus has previously been used to determine the differential cross section (28) of the inelastically scattered NO molecules in NO + Ar collisions. A pair of doubly skimmed pulsed free-jet expansions forms well collimated molecular beams that intersect at $\sim 90^\circ$ (Fig. 1).⁵ One of the beams is pure Ar, the other a mixture of 5% NO in Ar, with NO molecules predominantly in the ground rovibrational state. Elastically and inelastically scattered NO products are observed by quantum state-selective ionization using ($1 + 1'$) resonance-enhanced multiphoton ionization (REMPI) through the $R_{21}(7.5)$ line of the NO ($A^2\Sigma \leftarrow X^2\Pi$) transition at 226.057 nm (29). The bandwidth of our excitation laser is sufficiently narrow to ensure that only those NO molecules in the $j' = 7.5$ state are excited to the $A^2\Sigma$ state and subsequently ionized by a 266-nm photon. The ions are formed in an electrostatic lens system (26) that focuses and directs them onto a microchannel plate detector with a phosphorescent screen. Images created on the detector are captured with a charge-coupled device (CCD) camera. Spatial positions in this image reveal the velocities of the scattered NO molecules being detected, with the velocity given by the ratio of the displacement on the detector, measured from the beam crossing point to the flight time of the ions from the laser-molecular beam intersection region to the detector, multiplied by an instrumental magnification factor.

To determine the absolute velocity of the scattered $\text{NO}_{7.5}$ molecules, we must establish accurately the origin of the laboratory coordinate system. We produced two effusive beams of $\text{NO}({}^2\Pi_{1/2}, j = 0.5)$ with a low-pressure mixture of 5% NO in Ar in both valves, and we recorded a velocity-mapped ion image. This image showed two diagonal streaks that mark the two-beam propagation axes. The intersection of the streaks is the origin in the laboratory frame of reference. The angle between the streaks is the intersection angle, which we determined experimentally to be 90.8° .

From a similar measurement using two supersonic molecular beams, we also measured the speed of the NO reactant [$594 \pm 8 \text{ m s}^{-1}$, with a spread of about 7% full-width at half-maximum (FWHM)] (30). Previous measurements with pure Ar expansions at these conditions have shown the speed to be within a few percent of the ideal value, with spreads of 5 to 10%. From these two speeds and the 90.8° intersection angle, we determined a relative collision velocity of $818 \pm 29 \text{ m s}^{-1}$ and a COM velocity of $404 \pm 21 \text{ m s}^{-1}$, oriented at 85.6° with respect to the relative velocity vector.

Here, the molecular beam conditions were selected to provide the velocity vector cancellation that results in scattered $\text{NO}_{7.5}$ at zero laboratory-frame velocity. The necessary conditions for this cancellation are readily established from Newtonian mechanics and vector algebra. The cancellation occurs when $\mathbf{u}'_{\text{NO}} = -\mathbf{v}_{\text{cm}}$, where \mathbf{u}'_{NO} is the COM frame recoil velocity of the scattered $\text{NO}_{7.5}$ and \mathbf{v}_{cm} is the velocity of the NO + Ar COM in the laboratory-frame coordinate system. Here we use the convention of primed variables to denote post-collision values, and unprimed variables for the pre-collision values. The velocity cancellation condition follows from the relation between the laboratory-frame velocity of the scattered NO, \mathbf{v}'_{NO} , and its COM frame counterpart: $\mathbf{v}'_{\text{NO}} = \mathbf{u}'_{\text{NO}} + \mathbf{v}_{\text{cm}}$. For simplicity, we separate the vector cancellation condition into two scalar conditions for \mathbf{u}'_{NO} , one for its magnitude and one for its direction. The former is most simply written as a constraint on energy

$$E'_{\text{int}}(\text{NO}_{v'=0}) = \left(1 - \frac{m_{\text{NO}}}{m_{\text{Ar}}}\right) \times E_{\text{trans}}(\text{NO}(j = 0.5)) \quad (1)$$

where m_{NO} and m_{Ar} are the masses of NO and Ar, and $E_{\text{trans}}(\text{NO}(j = 0.5))$ is the lab-

frame translational energy of the NO in the molecular beam. $E'_{\text{int}}(\text{NO}_{v'=0})$ is the amount of energy that must be deposited into the internal modes of the NO molecule in order to produce molecules that are stationary in the laboratory frame of reference. On inspection, it may seem surprising that only the energy of the NO and not that of Ar appears in this constraint; however, this outcome is a direct consequence of the separation of the vector constraint into two scalar constraints.

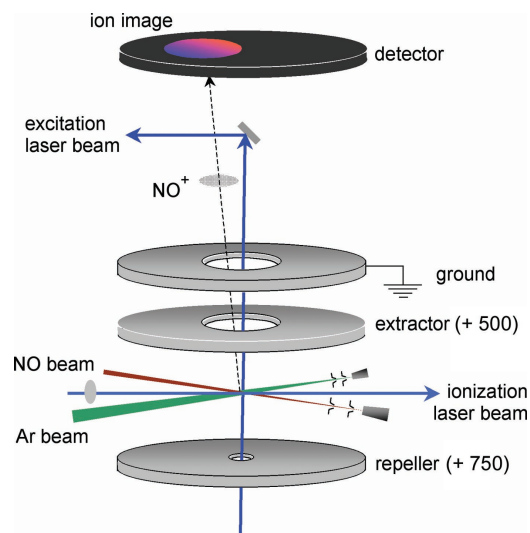
The condition for the scattering angle that must be met in order for the NO to have zero laboratory-frame velocity is

$$\cos(\Theta_{\text{cm}}) = \frac{E_{\text{Ar}} - E_{\text{NO}}}{\sqrt{\left(E_{\text{NO}} + \frac{m_{\text{NO}}}{m_{\text{Ar}}} E_{\text{Ar}}\right) \left(E_{\text{NO}} + \frac{m_{\text{Ar}}}{m_{\text{NO}}} E_{\text{Ar}}\right)}}, \quad (2)$$

where E_{NO} and E_{Ar} are the kinetic energies of NO and Ar, respectively. Because the angular distribution of the inelastically scattered $\text{NO}_{7.5}$ is quite broad, this condition is easy to establish, and it is indeed established for our experimental conditions. More generally, one can select the translational energy of the NO beam such that $|\mathbf{u}'_{\text{NO}}|$ matches a desired quantum state and select the translational energy of the Ar beam to ensure that sufficient scattering events satisfy the angular condition.

An interesting consequence of Eq. 1 for the scattering of partners with identical masses (D_2 colliding with He, for instance) is that the amount of internal energy for scattered molecules satisfying the zero-velocity condition is zero; i.e., the scattering is elastic. Under this condition, the velocity spread is identically zero because of all elastic scattering products must lie on a Newton sphere that intersects the origin, regardless of collision energy. Those scattered in the appropriate

Fig. 1. Diagrammatic illustration of the crossed molecular beam apparatus showing the $1 + 1'$ REMPI probe laser beams and ion imaging. Doubly skimmed NO and Ar beams intersect at a right angle which is bisected by the ionization laser beam. The excitation laser beam is propagated perpendicular to the scattering plane in order to minimize Doppler broadening due to a non-zero velocity distribution in the molecular beams. Velocity-mapped ion optics (repeller and extractor) focus the ionized $\text{NO}({}^2\Pi_{1/2}, j' = 7.5)$ scattering products toward the position-sensitive detector, which consists of a pair of chevron-type microchannel plates (MCP) and a phosphor screen. This two-dimensional projection of the scattered products is collected using a CCD camera and transferred to a computer for analysis.



REPORTS

direction will be completely stationary in the laboratory, and one can choose a collision energy that optimizes scattering amplitude in that direction.

In the false-color image of $\text{NO}_{7.5}$ from $\text{NO}({}^2\Pi_{1/2}, j = 0.5) + \text{Ar} \rightarrow \text{NO}({}^2\Pi_{1/2}, j' = 7.5) + \text{Ar}$ (Fig. 2),² the scattered $\text{NO}_{7.5}$ lies on a circle with a radius corresponding to its COM recoil velocity of $411 \pm 10 \text{ m s}^{-1}$, associated with $2.53 \pm 0.12 \text{ kJ mol}^{-1}$ of product translational energy for this state at the total relative collision energy of $5.73 \pm 0.20 \text{ kJ mol}^{-1}$. The center of the scattering circle is the origin of the COM coordinate system. This origin is translated with respect to the origin of the laboratory-frame coordinate system, which is the intersection of the NO and Ar beams, by a distance that corresponds to the velocity of the COM of the NO + Ar system. The NO molecular beam contains a small amount of $\text{NO}_{7.5}$ not cooled in the expansion, which is seen as a small diagonal band of intensity intersecting the circle of scattered $\text{NO}_{7.5}$ on the left side of the image at $\theta = 0^\circ$. On the circle of scattered $\text{NO}_{7.5}$ product, a very intense and sharp peak is observed near the top of the circle ($\theta = 85.6^\circ$ in the COM-frame coordinate system). This peak is at the origin of the laboratory frame and therefore near-zero laboratory velocity and arises from $\text{NO}_{7.5}$ produced by scattering of $\text{NO}_{0.5}$ from an argon atom. Residual $\text{NO}_{7.5}$ in the molecular beam, if elastically scattered, will have a faster velocity.

Our NO molecular beam has a translational energy of $5.29 \pm 0.26 \text{ kJ mol}^{-1}$. For this translational energy, Eq. 1 states that an internal energy in the NO of $1.32 \pm 0.07 \text{ kJ mol}^{-1}$ is required for an NO molecule to

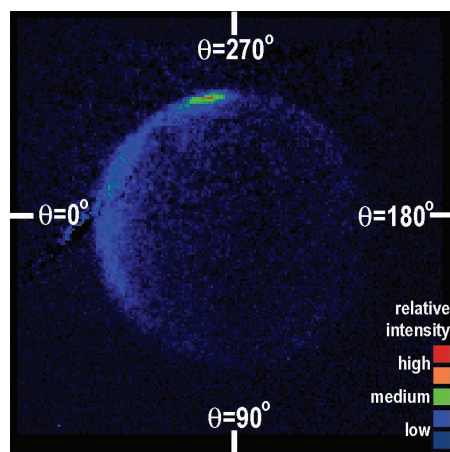


Fig. 2. Velocity-mapped ion image for collisions between NO and Ar, $\text{NO}({}^2\Pi_{1/2}, j = 0.5) + \text{Ar} \rightarrow \text{NO}({}^2\Pi_{1/2}, j' = 7.5) + \text{Ar}$ at a COM collision energy of $5.73 \pm 0.20 \text{ kJ mol}^{-1}$. The intense spot at the top of the scattering sphere is the result a collapse of the velocity spreads of the molecular beams for those molecules whose scattered velocity vector cancels the COM velocity of the collision pair.

become stationary upon colliding with an Ar atom. The rotational energy of NO in the $j = 7.5$ quantum state is $1.297 \text{ kJ mol}^{-1}$. Because the energy spread in the NO beam is larger than the energy mismatch, $\text{NO}_{7.5}$ molecules that are scattered in the correct direction, given by Eq. 2 above, will be nearly stationary in the laboratory frame.

We determine the density of these cold $\text{NO}_{7.5}$ molecules to be 10^8 to 10^9 molecules cm^{-3} by comparing the absolute intensity at the origin in the image shown in Fig. 2 with the image from a sample of thermal NO at known temperature and density. A measure of the production efficiency can be introduced upon consideration of three factors: the percentage of molecules in the molecular beam that suffer collisions with Ar, the portion of collisionally scattered $\text{NO}_{7.5}$ molecules whose velocities are less than 15 m s^{-1} , and the fraction of NO scattering into $j' = 7.5$ relative to scattering into other states. In our experiments, $\sim 1\%$ of the NO molecules collide with Ar atoms. By comparison of the integral collision cross sections (31) for scattering into all energetically accessible rotational states of NO via collisions with Ar, we estimate that 6% of the NO molecules end up in $j' = 7.5$. Finally, the ratio of the integrated intensity in the near-zero velocity region from the image shown in Fig. 2 to the integrated intensity over the entire scattering sphere is 0.016. Combining these multiplicative factors, we see that the fraction of NO molecules in the beam that are cooled is approximately 10^{-5} .

Figure 3 shows a profile across the spike of intensity at $v'_{\text{NO}} = 0$ on the raw data. The data are a two-dimensional (2D) projection of the 3D distribution of scattered products, and there is no reason that the resulting velocity distribution should obey Boltzmann statistics. According to Eq. 1, it should reflect the approximately Gaussian velocity spread in the NO molecular beam. We fit the intensity

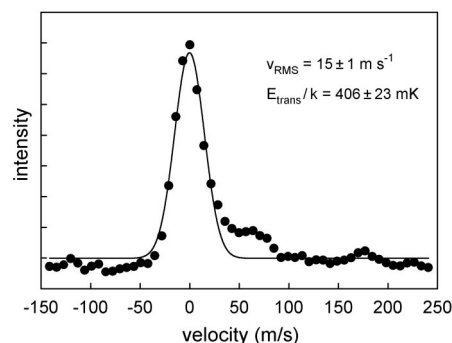


Fig. 3. The in-plane velocity distribution of NO (${}^2\Pi_{1/2}, j' = 7.5$) from the inelastic scattering $\text{NO}({}^2\Pi_{1/2}, j = 0.5) + \text{Ar} \rightarrow \text{NO}({}^2\Pi_{1/2}, j' = 7.5) + \text{Ar}$. The curve is a fit of the data to a Gaussian distribution function, with a temperature of $406 \pm 23 \text{ mK}$. The velocity distribution is a maximum at zero and has a RMS velocity of 15 m s^{-1} .

distribution to the form

$$f(v) = A e^{-\frac{1}{2} \left(\frac{v - v_0}{b} \right)^2} \quad (3)$$

The fit yields a RMS velocity of $15 \pm 1 \text{ m s}^{-1}$, and a half-width at half maximum (HWHM) velocity of $18 \pm 1 \text{ m s}^{-1}$. By convention and for the purpose of comparison to the results of other researchers, we report the temperature as the ratio of $E_{\text{trans}}(\text{NO}_{7.5})/k = 406 \pm 23 \text{ mK}$, where k is Boltzmann's constant. These are velocity and temperature conditions for which trapping and cooling the NO molecules is feasible. For the purpose of comparison to other techniques (11), we calculate the phase space density, or degeneracy parameter, $D = n\lambda^3$ to be 1×10^{-19} . Here, the number density of $\text{NO}_{7.5}$ is $n = 9 \times 10^8$ molecules cm^{-3} and the thermal deBroglie wavelength (λ) of NO at 406 mK is $\sim 5 \times 10^{-10} \text{ m}$; is defined by $\lambda = h/(2\pi mkT)^{1/2}$. We estimate that the original molecular beam with a translational temperature of 4 K has a degeneracy parameter of approximately 10^{-30} for $\text{NO}_{7.5}$. Thus, we have substantially increased the phase space density of $\text{NO}_{7.5}$.

We can predict the distribution in the laboratory-frame velocity of the translationally cold NO caused by the spread in the velocities of the NO and Ar beams with a simple analysis of the behavior of $\mathbf{v}'_{\text{NO}} = \mathbf{u}'_{\text{NO}} + \mathbf{v}_{\text{cm}}$ around $\mathbf{u}'_{\text{NO}} = -\mathbf{v}_{\text{cm}}$ that characterizes the cold molecules. To first order, the spread in v'_{NO} does not depend on the spread in v_{Ar} , as Eq. 1 would indicate should be the case. The dependence on the spread in v_{NO} is interesting as it shows a kinematic compression of the velocity spread. We have

$$\Delta v'_{\text{NO}} = \left(\frac{v_{\text{NO}}}{v_{\text{cm}}} \right) \left(\frac{m_{\text{Ar}}^2 - m_{\text{NO}}^2}{(m_{\text{Ar}} + m_{\text{NO}})^2} \right) \Delta v_{\text{NO}} = 0.21 \Delta v_{\text{NO}} \quad (4)$$

Our NO beam has a velocity spread (HWHM) of 21 m s^{-1} , so the distribution of v'_{NO} around $v'_{\text{NO}} = 0$ has a width (HWHM) of only 4.4 m s^{-1} . This value represents the limit on the temperature of our cold NO that can be achieved with our current NO beam source and gives $T = E_{\text{trans}}/k = 35 \text{ mK}$. This compression is the reason that, even with the broadening due to ion imaging detection of the scattered NO, we see a v'_{NO} distribution that is substantially narrower than the velocity spread in the NO beam itself. This results from the cancellation of the variation in v_{NO} due to its similar influence on both \mathbf{u}'_{NO} and \mathbf{v}_{cm} , just as the cancellation of \mathbf{u}'_{NO} and \mathbf{v}_{cm} leads to a most probable v'_{NO} of zero.

The NO molecules produced may indeed be this cold, but our apparatus does not allow us to resolve NO velocities associated with such a low temperature. Production of NO beams with narrower velocity spreads is pos-

sible, so this limit can be reduced. As noted earlier when discussing Eq. 1, for molecular collisions in which the masses of the two particles are equal, the contribution of the spread in both beam velocities to the velocity distribution of the scattered molecules vanishes to first order.

The measured RMS velocity spread, 15 m s^{-1} , is greater than three times that predicted by Eq. 4. Our measured velocity spread of cold NO molecules is an upper limit to the actual spread in velocities, as is the temperature associated with this velocity spread. In our experiment, there are several sources that broaden the reported velocity distribution. First is the resolution of the microchannel plate detector and camera, about 8 m s^{-1} . Second, the resolution of the velocity mapping itself can be compromised by charge repulsion of the ions and imperfect ion optics. From measurement of parent ions in our molecular beams, we estimate this to add approximately 10 m s^{-1} of velocity spread. Third is the velocity imparted to the detected NO^+ ions by the recoil of the electron from the NO^+ upon two-photon ionization that creates the NO^+ we detect. The recoiling photoelectron imposes a velocity spread of approximately 10 m s^{-1} . A fourth source of broadening comes from the nature of the measurement, which is a projection of the 3D spherical velocity distribution onto the 2D detector. Scattering above and below the scattering plane gives rise to the asymmetric tail on the distribution of Fig. 3. These sources of broadening in the measured NO velocity distribution account for a substantial fraction of the observed width of the measured distribution.

The vector constraint that must be satisfied to produce zero-velocity molecules, $\mathbf{u}'_{\text{NO}} = -\mathbf{v}_{\text{cm}}$, can readily be satisfied. It represents two independent scalar constraints in a system in which (for fixed beam intersection angle) there are three experimental variables—the energies of the two colliding molecules and the ratio of their masses—whose values can be selected to achieve that condition. For producing zero-velocity species AB, the AB energy can be adjusted by changing the temperature of the AB free-jet expansion nozzle and the diluent gas in which it is seeded. The energy of the collider species can be selected by the temperature of its free-jet expansion nozzle, and because the chemical identity of the collider species is not important, the ratio of the masses can be readily selected.

References and Notes

1. C. E. Weiman, D. E. Pritchard, D. J. Wineland, *Rev. Mod. Phys.* **71**, S253 (1999).
2. M. H. Anderson, J. R. Ensher, M. R. Matthews, C. E. Wieman, E. A. Cornell, *Science* **269**, 198 (1995).
3. C. C. Bradley, C. A. Sackett, J. J. Tollett, R. G. Hulet, *Phys. Rev. Lett.* **75**, 1687 (1995).

4. K. B. Davis *et al.*, *Phys. Rev. Lett.* **75**, 3969 (1995).
5. S. L. Rolston, W. D. Phillips, *Nature* **416**, 219 (2002).
6. K. Burnett, P. S. Julienne, P. D. Lett, E. Tiesinga, C. J. Williams, *Nature* **416**, 225 (2002).
7. S. A. Diddams *et al.*, *Science* **293**, 825 (2001).
8. A. Kerman, V. Vuletic, C. Chin, S. Chu, *Phys. Rev. Lett.* **84**, 439 (2000).
9. C. Monroe, W. Swann, H. Robinson, C. Wieman, *Phys. Rev. Lett.* **65**, 1571 (1990).
10. W. Ketterle, *Int. J. Mod. Phys.* **16**, 4537 (2002).
11. H. L. Bethlem, G. Meijer, *Int. Rev. Phys. Chem.* **22**, 73 (2003).
12. F. Masnou-Seeuws, P. Pillet, *Adv. Atom. Mol. Opt. Phys.* **47**, 52 (2001).
13. J. T. Bahns, P. L. Gould, W. C. Stwalley, *Adv. Atom. Mol. Opt. Phys.* **42**, 171 (2000).
14. J. P. Shaffer, W. Chalupczak, N. P. Bigelow, *Phys. Rev. A* **63**, 021401 (2001).
15. H. R. Thorsheim, J. Weiner, P. S. Julienne, *Phys. Rev. Lett.* **58**, 2420 (1987).
16. T. Takekoshi, B. M. Patterson, R. J. Knize, *Phys. Rev. Lett.* **81**, 5105 (1998).
17. J. D. Miller, R. A. Cline, D. J. Heinzen, *Phys. Rev. Lett.* **71**, 2204 (1993).
18. E. A. Donley, N. R. Clausen, S. T. Thompson, C. E. Wieman, *Nature* **417**, 529 (2002).
19. C. A. Regal, C. Ticknor, J. L. Bohn, D. S. Jin, *Nature* **424**, 47 (2003).
20. J. D. Weinstein, R. deCarvalho, T. Guillet, R. Friedrich, J. M. Doyle, *Nature* **395**, 148 (1998).
21. J. Kim *et al.*, *Phys. Rev. Lett.* **78**, 3665 (1997).
22. H. L. Bethlem *et al.*, *Nature* **406**, 491 (2000).
23. H. L. Bethlem, G. Berden, A. J. A. van Roij, F. M. H. Crompvoets, G. Meijer, *Phys. Rev. Lett.* **84**, 5744 (2000).
24. M. Gupta, D. Herschbach, *J. Phys. Chem. A* **103**, 10670 (1999).
25. M. S. Westley, K. T. Lorenz, D. W. Chandler, P. L. Houston, *J. Chem. Phys.* **114**, 2669 (2001).
26. D. W. Chandler, D. H. Parker, in *Advances in Photochemistry*, D. C. Neckers, D. H. Volman, Eds. (Wiley, New York, 1999), vol. 25.
27. T. J. B. Eppink, D. H. Parker, *Rev. Sci. Instr.* **68**, 3477 (1997).
28. M. S. Eliofo, D. W. Chandler, *J. Chem. Phys.* **117**, 6455 (2002).
29. J. Luque, D. R. Crosley, LIFBASE: Database and Simulation Program (v. 1.6), SRI International Report No. MP99-109 (SRI International, Menlo Park, CA, 1999).
30. The error bars reflect uncertainty in our measurement of the mean velocity and are derived by propagation of errors using standard rules. The spread reflects the width of the statistical distribution of velocities in the supersonic molecular beam of NO molecules. We did not measure the speed of the Ar beam; we used the computed value for an ideal isentropic expansion, 554 m s^{-1} , and assumed a spread of 7% FWHM.
31. M. H. Alexander, *J. Chem. Phys.* **111**, 7426 (1999).
32. We thank M. Jaska and B. Parsons for the considerable insight and assistance they provided during the course of this research. Funding for this work was provided by the U.S. Department of Energy, Office of Basic Energy Science, Division of Chemical Sciences, Geosciences, and Biosciences. Sandia is a multiprogram laboratory operated by Sandia Corporation, a Lockheed Martin Company, for the U.S. DOE's National Nuclear Security Administration under contract DE-AC04-94AL85000.

21 August 2003; accepted 6 November 2003

Importance of Surface Morphology in Interstellar H_2 Formation

L. Hornekaer,^{1*} A. Baurichter,¹ V. V. Petrunin,¹ D. Field,²
A. C. Luntz¹

Detailed laboratory experiments on the formation of HD from atom recombination on amorphous solid water films show that this process is extremely efficient in a temperature range of 8 to 20 kelvin, temperatures relevant for H_2 formation on dust grain surfaces in the interstellar medium (ISM). The fate of the 4.5 electron volt recombination energy is highly dependent on film morphology. These results suggest that grain morphology, rather than the detailed chemical nature of the grain surface, is most important in determining the energy content of the H_2 as it is released from the grain into the ISM.

The formation of molecular hydrogen in interstellar molecular clouds is the key first step in both the formation of stars and in the evolution of molecular complexity in the interstellar medium (ISM). It is widely accepted that (i) there is no efficient gas phase route for H_2 formation from H atoms at the low temperatures and densities of the ISM and (ii) H_2 is formed by H atom recombination on dust grains that are integrally associated with the interstellar molecular clouds (1). To account for the astronomi-

cally observed H_2 formation rate in clouds (2, 3), the surface recombination of H atoms on grains to produce H_2 must be a very efficient process at $T \sim 10 \text{ K}$ (1). However, previous laboratory experiments on H_2 formation on surfaces of astrophysical relevance were interpreted as implying that the recombination is thermally activated (4), requiring $T \geq 20 \text{ K}$ (5) for surfaces thought to be important in dark interstellar clouds. The formation of each H_2 molecule also releases 4.5 eV of energy. How this energy is partitioned amongst the various degrees of freedom is crucial in understanding the temporal and chemical evolution of molecular clouds (6). For example, partitioning of the reaction energy into H_2 kinetic energy heats the cloud, while vibrational excitation of the H_2 or

¹Department of Physics, University of Southern Denmark, Denmark. ²Department of Physics and Astronomy, Aarhus University, Denmark.

*To whom correspondence should be addressed. E-mail: hornekaer@fysik.sdu.dk